Effect of High-Range Water-Reducing Admixtures on Alkali-Activated Slag Concrete

Sun, Yubo; Tao, Yaxin; Rahul, A. V.; Ye, Guang; De Schutter, Geert

DOI
10.14359/51737192

Publication date
2022

Document Version
Final published version

Published in
ACI Materials Journal

ACI MATERIALS JOURNAL TECHNICAL PAPER

Title No. 119-M124

Effect of High-Range Water-Reducing Admixtures on Alkali-Activated Slag Concrete

by Yubo Sun, Yaxin Tao, A. V. Rahul, Guang Ye, and Geert De Schutter

The rapid workability loss of alkali-activated materials (AAMs) has been a major obstacle limiting their on-site application. In this study, two conventional high-range water-reducing admixtures (HRWRAs) (made of polynaphthalene sulfonate [PNS] and lignosulfonate [LS] salts), which have been reported to be effective in some specific AAM mixtures, were separately applied in alkali-activated slag (AAS) concretes. A comprehensive testing program was performed to study their effect on reaction kinetics, rheology evolution, and strength development. Results showed that sodium silicate-activated AAS mixtures exhibited lower yield stress than those activated by sodium hydroxide. In hydroxide media, PNS and LS remained effective in reducing yield stress and increasing slump value, while they both failed to improve the rheological behavior of AAS activated by silicate. Moreover, the inclusion of 2% admixtures did not result in much strength reduction in either activator, although LS showed a retardation effect and subsequent increase in the setting time in the fresh state.

Keywords: alkali-activated slag (AAS) concrete; high-range water-reducing admixture (HRWRA); reaction kinetics; rheology; strength development.

INTRODUCTION

During the last decades, numerous studies have been conducted trying to find an eco-friendly alternative binding material for concrete structures, because the production of portland cement (PC) clinker is associated with heavy energy consumption and pollutant emission.[1] Alkali-activated material (AAM) is regarded as one of the most promising alternatives, which shows comparable or even better mechanical properties and durability than PC materials.[2]

The alkali-activation reaction takes place between aluminosilicate precursors and alkaline activators. In recent years, more innovative raw materials from local waste streams have been involved as a supplement to the existing precursors.[3-5] The availability of mainstream precursors will be turned localized, depending on the policies in different regions of the world (for instance, the production of fly ash and steel slag could be affected due to the coal phase-out[6] and green steel production,[7] respectively). By using various industrial waste and by-products as precursors, AAM significantly reduces CO_2 emissions from clinker calcination over traditional cement production. However, it is a concern that the application of highly concentrated alkaline substances will, on the other hand, induce environmental impact, especially the sodium silicate, which is produced through high temperature and pressure processes.[8] Nevertheless, Turner and Collins[9] suggested that the reduction in CO_2 emission by substituting PC binders with AAMs ranges between 9 and 80%, while in some cases, the contributions from treatment, transportation, curing, and so on were not considered.

Apart from that, the workability issue[10-12] is one of the most prominent drawbacks limiting the on-site application of AAM concrete. For instance, after mixing, there is insufficient time for delivering, casting, and compacting.[13] Unlike PC materials, where water is applied as a universal solvent, a certain amount of alkaline substances should be pre-dissolved into the solvent (that is, the activator) to promote the dissolution of precursors because they are insufficiently reactive.[14-16] Regarding the properties of AAM and industrial relevance, sodium silicate and sodium hydroxide are the most commonly used activators,[2] and both of them would increase the viscosity of aqueous solutions when dissolved in water.[2,17] Moreover, the silicate species, as one of the major reactants forming both calcium aluminosilicate hydrate (C-A-S-H) and sodium aluminosilicate hydrate (N-A-S-H) polymerization products,[18,19] are semi-provided by the solvent when sodium silicate is applied as the activator, which makes the reaction kinetics in AAM rather complex. In addition, the type and amount of alkaline substances involved in the activator play a major role in the property of the activator, as well as the rheology and reaction mechanism of AAM mixtures.

In alkali-activated slag (AAS) systems, rapid setting and loss of workability have been frequently reported, especially when silicate is applied in the activator.[11,20,21] The reaction mechanism has been extensively investigated, especially at the early stage, to better understand the setting behavior of AAS. It is generally accepted that the nature of the activator has a major impact on the reaction process.[22-24] Such uncontrolled behavior is attributed to the rapid accumulation of primary C-(A)-S-H gel,[11,13,22,25] which is the intermediate product from the reaction between the calcium dissolved from slag particles and the silicate species originating from the activator.

In PC materials, several generations of plasticizers and water-reducing admixtures have been developed to better disperse cement particles through electrostatic repulsion and steric hindrance.[26,27] Meanwhile, studies have been conducted to try to improve the rheology of AAM by using conventional high-range water-reducing admixtures (HRWRAs).[25,28-37] Unfortunately, only polynaphthalene sulfonate (PNS) and lignosulfonate (LS)-based HRWRAs have been reported to be stable and remained effective in some specific AAM mixtures.[25,30,31,34-36] In general, the

ACI Materials Journal, V. 119, No. 6, November 2022.
MS No. M-2022-074.R2, doi: 10.14359/51737192, received June 29, 2022, and reviewed under Institute publication policies.

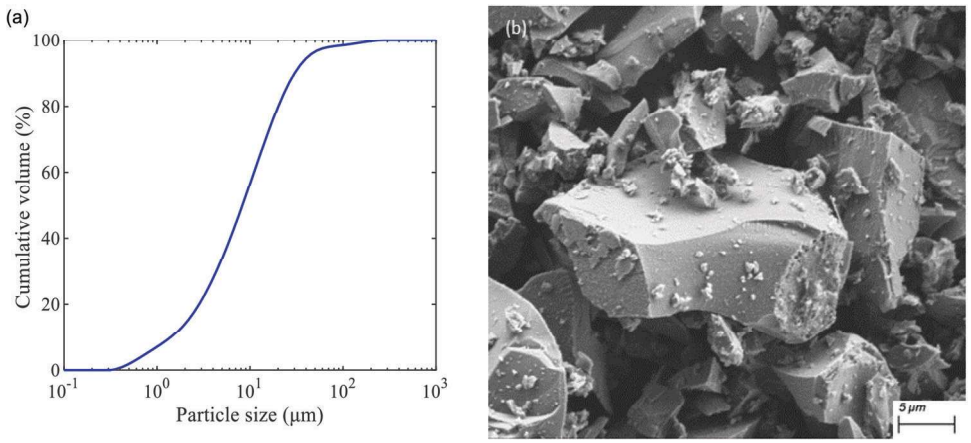

Fig. 1—Physical properties of slag cement: (a) particle-size distribution; and (b) morphology by SEM. (Note: 1 μm = 3.9 × 10^{-5} in.)

Table 1—Chemical composition of slag cement measured by XRF and LOI, mass %

Precursor	CaO	SiO_2	Al_2O_3	MgO	SO_3	TiO_2	K_2O	Fe_2O_3	MnO	ZrO_2	Other	LOI*
Slag cement	40.9	31.1	13.7	9.16	2.31	1.26	0.69	0.40	0.31	0.12	0.05	0.10

*LOI measured by thermogravimetric analysis (TGA) at 1742°F (950°C).

majority of conventional HRWRAs became less effective or even totally ineffective in AAM mixtures. In some extreme cases, attempts have been made to improve the fresh properties of AAM by using a rather high-dosage HRWRA; however, few of them succeeded, while significant strength reduction was reported.[38,39] It was concluded by many researchers that the effectiveness of HRWRAs in AAM systems primarily depends on their stability in highly alkaline media.[35,40,41]

The fresh properties of AAM mixtures are also affected by other factors, for instance, the nature of precursors and activators, as well as the dosage of HRWRAs and the affinity between the HRWRA and precursor particles.[33] Palacios et al.[25] studied the adsorption of HRWRAs in PC and AAS systems. Opposite zeta potential was detected in PC (+5 mV) and AAS (–2 mV) suspensions. Accordingly, the negatively charged HRWRAs could not effectively adsorb on slag particles, so their adsorption is significantly lower than on PC by a factor between 3 and 10. Similar properties have been detected in fly ash and metakaolin-based mixtures as well.[42,43] Marchon et al.[44] proposed that the lower effectiveness of HRWRAs was due to competitive adsorption between HRWRAs and the silicates originating from the activators. Palacios et al.[33,35] also reported that PNS stayed stable in highly concentrated sodium hydroxide but suffered structural changes with the presence of sodium silicate, while structural changes in functional groups of other HRWRAs were detected at pH > 13. More relevant research is needed to get a fundamental understanding of the working mechanism of HRWRAs in AAM systems.

The current study performed a comprehensive investigation of the effect of conventional HRWRAs (PNS and LS) on AAS concrete in both hydroxide and silicate media. The effect of both HRWRAs on the reaction kinetics was evaluated by calorimetry. Meanwhile, the fresh properties of the different mixtures were characterized by the slump loss and rheological parameters (derived from the stress growth test and flow curve test with a concrete rheometer) over time. Furthermore, the compressive strength of hardened samples at different curing ages was also evaluated. The results obtained from this study illustrate the possibility of producing AAS concrete with conventional HRWRAs.

RESEARCH SIGNIFICANCE

In previous literature, the rheological study of AAM is still limited, and most researchers merely focused on paste and mortar levels. Rheological data of AAM concrete so far in published studies are still scarce. The objective of this study is to upscale the current knowledge about the effect of HRWRAs on AAS paste and mortar in concrete mixtures, and further evaluate the rheological and mechanical properties of AAS concrete. The authors believe that this detailed study dealing with the effect of conventional HRWRAs on the fresh and hardened properties will be very useful to the applications of AAS concrete.

EXPERIMENTAL INVESTIGATION

Materials

The slag cement used in this study had a density of 180.42 lb/ft^3 (2890 kg/m^3). The particle-size distribution measured by laser diffraction is given in Fig. 1(a), and the d_{50} is 3.26 × 10^{-4} in. (8.28 μm). The morphology of the slag cement particles was observed with a scanning electron microscope (SEM), as shown in Fig. 1(b). Details of the chemical composition of the slag cement determined by X-ray fluorescence (XRF) and loss on ignition (LOI) are listed in Table 1.

Two types of alkaline compounds were applied as activators in this study, namely sodium hydroxide and sodium silicate. Reagent-grade sodium hydroxide anhydrous pearls were used, and the sodium silicate solution was 15% Na_2O, 30% SiO_2, and 55% water.

Two types of market-available HRWRAs that might be able to improve workability were applied in the AAS concretes. PNS and LS had 40% solid content in both HRWRAs.

River sand and gravel were used as the fine and coarse aggregates in this study. The physical properties of each fraction are listed in Table 2. The aggregates were air-dried to prepare the AAS concrete mixtures.

Mixture proportions

Details of the six different AAS concrete mixtures are given in Table 3. The reference mixture AAS1 was adapted from the high-strength slag concrete developed by the International Union of Laboratories and Experts in Construction Materials, Systems and Structures (RILEM) TC 247-DTA,[45] which was prepared with a sodium silicate activator. To study the effect of different activators, AAS2 was designed as a mixture with pure hydroxide activation. In AAS2, the silicate content was excluded from the activator, while the equivalent Na_2O content was kept constant as AAS1 by adding extra sodium hydroxide. In addition, AAS3 and AAS4 were designed to assess the effect of PNS in silicate and hydroxide systems, while LS was applied in AAS5 and AAS6 parallelly. The aggregate packing was designed to reach between the A16 and B16 curves indicated in DIN 1045-2. In each concrete mixture, the slag content was fixed at 23.41 lb/ft^3 (375 kg/m^3), and the aggregate-to-paste mass ratio was kept constant.

Depending on the nature of the activators applied, PNS and LS admixtures have been reported effective in some specific cases.[25,36,46] Thereby, it was decided to apply PNS and LS in this study to assess their effects on AAS concretes. It has been reported that both HRWRAs turned much less effective in silicate media,[12] even with high dosages. On the other hand, segregation of concrete was observed in trial batches, while the concentration of both HRWRAs exceeded 2% (by mass of slag cement) in hydroxide-based mixtures; similar results have been also reported in previous studies.[25] Thereby, the HRWRA dosage was fixed at 2% in this study to assess their effects in hydroxide and silicate systems. The water-binder ratio (w/b) was kept constant at 0.382 by compensating for the water content in the sodium silicate solutions and HRWRAs.

Table 2—Physical properties of aggregates

Aggregate	Sand 0 to 0.16 in. (0 to 4 mm)	Coarse 0.08 to 0.31 in. (2 to 8 mm)	Coarse 0.31 to 0.63 in. (2 to 8 mm)
Specific gravity	2.65	2.64	2.67
Water absorption, %	0.33	0.65	0.55

Testing program

In this study, the effect of HRWRAs on the reaction kinetics of AAS was investigated with the equivalent paste fraction as presented in Table 3, while the fresh properties and strength development of the AAS mixtures were measured at the concrete level.

In each mixture, the alkaline activator solutions were prepared 24 hours before mixing. Sodium hydroxide pearls and sodium silicate solution were dissolved in tap water. Eventually, the activator was sealed and cooled down to room temperature.

The AAS pastes were prepared with a mixer by mixing slag cement with the activators at a low speed (140 rpm) for 60 seconds. Afterward, the HRWRAs were added, and the AAS paste was further mixed at a high speed (285 rpm) for 90 seconds.

The heat evolution during the reaction process was monitored with an isothermal calorimeter. After mixing, 0.49 oz. (14 g) paste samples were immediately placed into glass ampoules. The ampoules were then sealed and loaded into the calorimeter, and the heat evolution was recorded at 68 ± 0.9°F (20 ± 0.5°C) for 24 hours. The initial setting times of the AAS pastes were determined by the Vicat needle apparatus according to EN 196-3.

The AAS concretes were prepared in a batch of 1.06 ft^3 (30 L) by following the same mixing protocol. The solid components (slag cement and aggregates) were first blended in the mixer for 2 minutes. Afterward, the activators and HRWRAs were added to the mixer and mixed for another 3 minutes. Finally, the fresh AAS concrete was divided into two groups. Approximately 0.71 ft^3 (20 L) of concrete was loaded into the rheometer container for rheological tests, while the rest was used for the slump test.

Table 3—Mixture proportions of AAS concretes

Mixture	Slag cement, kg/m^3	Activator, kg/m^3		Na_2O†	Admixture†	w/b‡	Aggregate, kg/m^3§		
		NaOH	$Na_2Si_2O_5$*				0 to 4 mm	2 to 8 mm	2 to 8 mm
AAS1	375	15	10.09	4%	0	0.382	729	503	590
AAS2	375	19.34	0	4%	0	0.382	728	502	589
AAS3	375	15	10.09	4%	2% PNS	0.382	729	503	590
AAS4	375	19.34	0	4%	2% PNS	0.382	728	502	589
AAS5	375	15	10.09	4%	2% LS	0.382	729	503	590
AAS6	375	19.34	0	4%	2% LS	0.382	728	502	589

*Represented in the form of $Na_2Si_2O_5$, as solid content in sodium silicate provided, has molar ratio of 2.

†Represented as mass percentage of slag cement.

‡Defined as water content in both aqueous activator and water added separately from activator divided by sum of precursor and solid activators.

§Designed to reach between A16 and B16 curves indicated in DIN 1045-2.

Note: 1 kg/m^3 = 0.0624 lb/ft^3; 1 mm = 0.039 in.

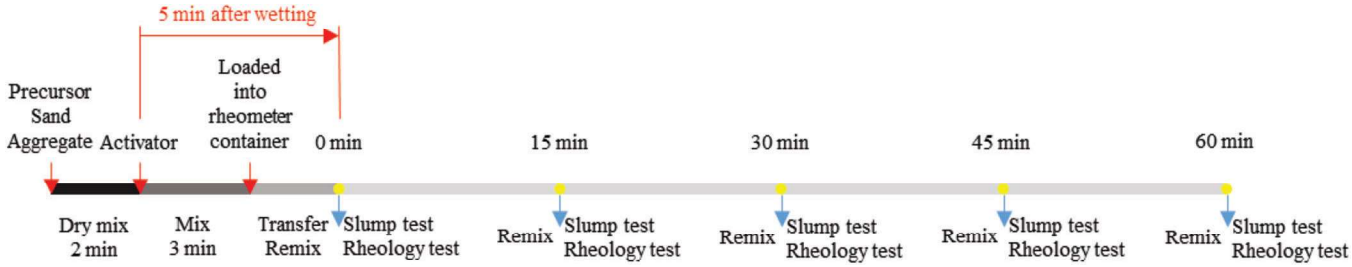

Fig. 2—Testing protocol for slump and rheology tests.

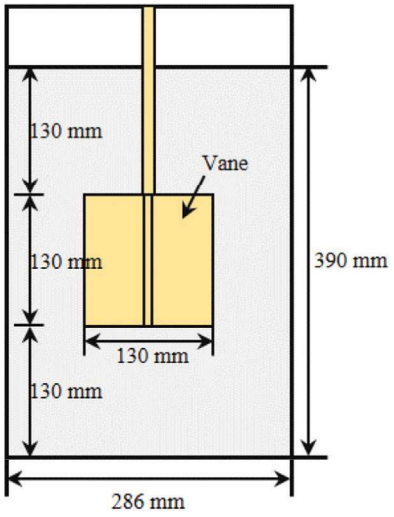

Fig. 3—Geometry of ICAR Plus rheometer. (Note: 1 mm = 0.039 in.)

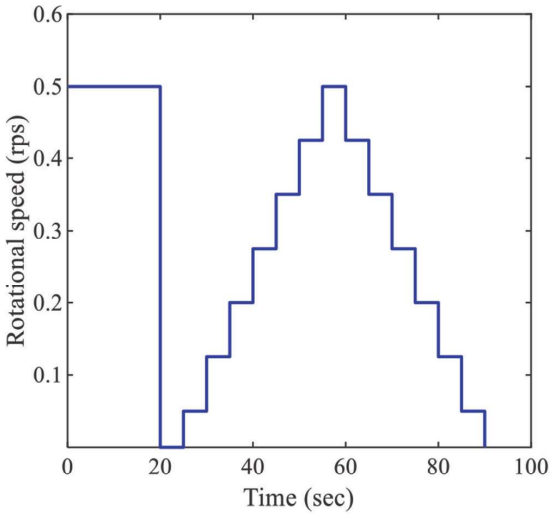

Fig. 4—Shear protocol used in flow curve test.

As illustrated in Fig. 2, the slump (according to EN 12350-2) and rheological tests were performed simultaneously to characterize the fresh properties of AAS concrete. The moment when the first group test started (5 minutes after wetting) was defined as 0 minutes. At each testing age, the concrete was remixed for 1 minute before the slump test.[47]

In parallel, the rheological parameters were determined by the stress growth and flow curve tests with the International Center for Aggregates Research (ICAR) Plus rheometer, fitted with a four-bladed vane (geometry is shown in Fig. 3). Before each group of tests, a 1-minute remixing with a handheld mixer was conducted to ensure consistent reference states among the different samples.[48] The vane was then immersed in the fresh mixture, and the AAS concrete was rested for 30 seconds to release the undissipated energy.[49] The stress growth test was first conducted with a constant rotational speed of 0.025 rev/s for 60 seconds. By applying a constant low shear rate, the torque responses first increased to the maximum and then progressively decayed until an equilibrium state. The static yield stress was determined from the peak torque according to Eq. (1),[50] indicating the energy required to break down the structuration.

$$\tau_0 = \frac{2T_m}{\pi D^3\left(\frac{h}{D}+\frac{1}{3}\right)} \quad (1)$$

where τ_0 is the static yield stress in Pa; T_m is the maximum torque in N·m; D is the diameter of the vane; and h is the height of the vane.

Subsequently, the flow curve test was carried out according to the shear protocol given in Fig. 4. For each flow curve test, a 20-second pre-shear was applied at 0.5 rev/s, followed by a 5-second rest. Afterward, shear was applied with stepwise increasing and decreasing rotational speed to derive the flow curves. The test was conducted for 5 seconds in each step, and the torque values were recorded to determine the rheological parameters.[50] Finally, the vane was removed at the end of the measurement, and the concrete was left at rest in the container until the next testing age. The downward portions of the torque-rotational speed relationship were linearly fitted based on the Bingham model to derive the flow curves. The dynamic yield stress and plastic viscosity were determined based on the Reiner-Riwlin equations (Eq. (2) and (3)).[50]

$$\tau_d = \frac{\left(\frac{1}{R_1^2}-\frac{1}{R_2^2}\right)}{4\pi h \ln\left(\frac{R_2}{R_1}\right)} G \quad (2)$$

$$\mu_p = \frac{\left(\frac{1}{R_1^2}-\frac{1}{R_2^2}\right)}{8\pi^2 h} H \quad (3)$$

where τ_d is the dynamic yield stress (Pa); μ_p is the plastic viscosity (Pa·s); R_1 is the radius of the vane (m); R_2 is the

radius of the rheometer container (m); G is the intercept of the descending flow curve in the torque-rotational relationship; and H is the slope of the flow curve in the torque-rotational relationship. Note that 1 m = 39.37 in.

Such experimental sequences of the slump, stress growth, and flow curve tests were repeated on the same batch of AAS concrete every 15 minutes in the first hour to study the fresh property evolution. After each group of tests, the concrete for the slump and rheology tests was recollected into separate containers and left at rest until the next testing age. The layer of remaining mixture attached to the testing devices (slump cone, rheometer vane, container walls, and so on) was scraped and collected to mitigate the influence of potential paste/mortar loss on testing results. During the rest period, the concrete was covered to prevent moisture evaporation.

After the fresh property measurements, the concrete was then cast into 3.94 in. (100 mm) cubic molds for the compressive strength test. Concrete cubes were demolded after 24 hours and sealed in plastic bags to prevent moisture evaporation and leaching of alkaline content. The specimens were placed in a curing chamber at 68°F (20°C), and the compressive strength was measured at 1, 7, 28, and 91 days according to EN 12390-3.

EXPERIMENTAL RESULTS AND DISCUSSION

Reaction kinetics

The heat flow and cumulative heat evolution of AAS paste, normalized per gram (0.04 oz.) of solid binder (including precursors and solid activators), are illustrated in Fig. 5(a) and (b), respectively. In both cases, the early-stage reaction

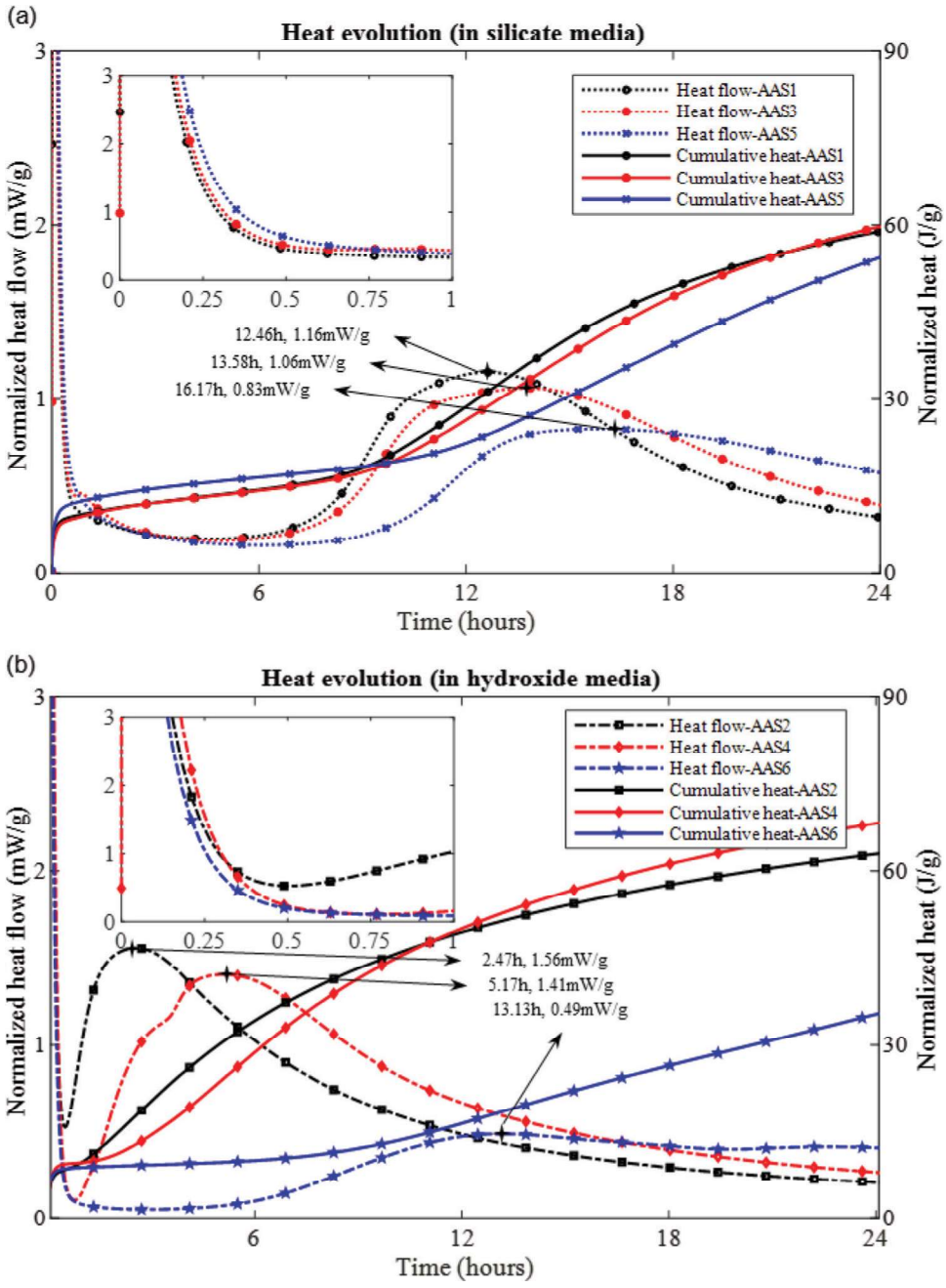

Fig. 5—Heat evolution of AAS pastes in: (a) silicate media; and (b) hydroxide media. (Note: 1 g = 0.04 oz.; 1 mW = 9.48 × 10^{-7} Btu/s; 1 J = 9.48 × 10^{-4} Btu.)

process is divided into five stages according to the heat evolution characteristics, namely: dissolution, induction, acceleration, deceleration, and the steady period, similar to the hydration features in PC materials.[51]

As presented in Fig. 5(a), referring to silicate activation, a very sharp peak was detected at the beginning of the heat flow measurements in all the mixtures, which represents the wetting and dissolution of slag particles right after mixing with activators.[52] Subsequently, a long induction period followed. The second exothermic peak, which reflects the acceleration and deceleration periods, occurred between 6 and 24 hours, with the peak value detected at approximately 12 hours. Eventually, the reaction reached a steady state, and the heat flow remained at a relatively low value. Two major increments were observed in cumulative heat evolution, corresponding to the two peaks in the heat flow measurements. The effect of the PNS-based HRWRA on the heat evolution in the silicate media was limited, with both the heat flow and cumulative heat curves of AAS1 and AAS3 almost identical. However, with the addition of 2% LS, the cumulative heat released during the dissolution period slightly increased, while the induction period was extended to approximately 8 hours. In addition to delaying the acceleration/deceleration peak, the height of this peak was decreased as well, which indicates that the reaction process was retarded by LS.

The calorimetry curves of the hydroxide-activated slag pastes are shown in Fig. 5(b). Compared to the reactions in the silicate media (Fig. 5(a)), the induction period was negligible, and the acceleration period was detected approximately 30 minutes after mixing in the heat flow measurement of AAS2. Moreover, the height of the second heat flow peak increased as well by using hydroxide under the same sodium oxide concentration in the activator, which means the exothermic reaction in the hydroxide media was faster and more intensive than in the silicate media. Regarding the effect of HRWRAs, both PNS and LS exhibited a more pronounced impact on heat evolution than in the silicate media. The initiation of the acceleration period was delayed from 30 to 55 minutes when 2% PNS was applied, and the greatest heat flow of the second exothermic peak was reduced by 9.6%. Furthermore, the cumulative heat released by AAS2 and AAS4 converged after approximately 12 hours and both reached approximately 65 J/g after 24 hours. In the case of 2% LS, significant retardation occurred when 2% LS was applied, the cumulative heat release declined approximately 50% after 24 hours, and the second exothermic peak after the induction period almost vanished.

In general, the presence of silicate in activators brought a significant impact on the heat evolution of AAS pastes. An obvious long induction period occurred when silicate was applied. Similar results can be found in References 16 and 52 to 54. The addition of silicate results in a relatively low Si gradient adjacent to the slag particles and thus inhibits the dissolution of Si.[55,56] Subsequently, a Si-rich layer is formed on the outer surface of undissolved slag particles[55] due to the progressive dissolution of Ca, Mg, and Al, so that the dissolution of these elements from inner slag particles are inhibited. In addition, a large amount of gel-like intermediate reaction products are formed due to the reaction between Ca, Al released from slag particles and silicates originating from the activator, wrapping around the unreacted slag particles and further blocking the contact between alkaline media and slag.[57] Accordingly, the dissolution and chemical reaction reach an equilibrium, and the heat evolution comes to the induction period. Afterward, the silicates provided by the activator are gradually consumed along with the continuous polymerization process,[58] the saturation of silicate is terminated, and silicate dissolved from slag particles is involved in the formation of reaction products.[23,57] Then the acceleration/deceleration period begins with another exothermic process in heat flow evolution until the reaction process reaches another equilibrium. In the AAS mixture made of sodium hydroxide (AAS2), the reaction took place very rapidly and the induction period was scarcely observed, which is in agreement with Ravikumar and Neithalath[52] and Altan and Erdoğan.[59] In addition, the intensity of the second exothermic peak also increased, which could be attributed to the high alkalinity.[11,52] In the silicate media (AAS3 and AAS5), the PNS admixture showed almost no impact on heat evolution, while LS delayed and reduced the peak value of the second exothermic peak in heat flow. However, in the case of hydroxide activation (AAS4 and AAS6), the second exothermic peak shifted rightward when both HRWRAs were applied. Meanwhile, there is a remarkable decrement in the cumulative heat by adding 2% LS, which revealed the strong retardation effect of LS.

The initial and final setting times of the AAS pastes are presented in Table 4. Compared to the reference mixture AAS1, the initial and final setting times significantly reduced (61% and 75%, respectively) in AAS2 with the hydroxide media. Regardless of the type of alkaline activator, both HRWRAs prolonged the initial and final setting times of the AAS paste, and the addition of LS resulted in more retardation than PNS.

Regarding PC materials, researchers have attempted to find the relationship between the setting behavior and heat evolution during the hydration process.[60,61] In this study, no straightforward correlation between setting time and heat evolution has been found within the AAS mixtures tested. Nevertheless, it is noteworthy that among the silicate-activated mixtures (AAS1, AAS3, and AAS5), all the initial setting times ranged within the induction period detected by calorimetry, while the initial setting of the hydroxide-activated pastes occurred after the acceleration period began. The result reveals that the hardening process in hydroxide and silicate media might be different. The setting behavior in the case of hydroxide activation is more like a PC material, where the precipitation of reaction products along with distinct exothermic behavior resulted in flocculation

Table 4—Initial and final setting times of AAS pastes

Setting time, minutes	AAS1	AAS2	AAS3	AAS4	AAS5	AAS6
Initial	155	60	315	120	450	315
Final	500	125	570	165	840	700

and binding of particles.[62,63] Meanwhile, the development of polymeric gel[64] was dominant in the setting of the silicate-activated mixtures to get the resistance against needle penetration in the Vicat test, and the heat evolution was insufficiently representative.

Fresh properties

Effect of HRWRAs on initial fresh properties—The flow curves in the torque-rotational speed relationship obtained at 0 minutes are presented in Fig. 6. In addition, the slump test and stress growth test were conducted on fresh concretes as well to determine the slump value and static yield stress, respectively. Results of the different AAS mixtures at 0 minutes are summarized in Fig. 7 to characterize their initial fresh properties.

As shown in Fig. 7, the AAS concretes made of silicate and hydroxide media exhibited very different initial fresh properties. It has been noticed that the static yield stress, dynamic yield stress, and plastic viscosity in AAS2 are significantly higher compared to AAS1, along with a remarkable reduction in slump value (60%) at 0 minutes. The result reveals that interactions between slag particles in the hydroxide media were much stronger than that in the silicate media so that stronger force to initiate flow, as well as higher resistance to flow,[65] were detected. In other words, the interaction between slag particles was mitigated with the presence of silicate in the activator, and the interparticle friction was reduced as the silicate and the preliminary gel products were wrapped around the slag particles.[57]

In the silicate media, the addition of HRWRAs showed very limited effects on initial fresh properties. At 0 minutes, 2% PNS and LS only improved the slump value by 11.4% and 8.6%, respectively. Regarding the rheological parameters, 2% PNS reduced the initial static and dynamic yield stress by 14.3% and 30.1%, respectively, while the plastic viscosity remained almost unchanged. Meanwhile, the inclusion of 2% LS slightly improved the static yield stress and reduced the plastic viscosity by 39.5%.

However, both HRWRAs remained rather effective in the hydroxide media. Two percent PNS and LS increased the slump value by 242.9% and 221.4%, respectively, compared to AAS2. An obvious decrement in rheological parameters has been detected as well in AAS4 and AAS6 compared to those in AAS2. Moreover, it is also noteworthy that PNS resulted in more reduction in static/dynamic yield stress, while LS led to more decline in plastic viscosity.

To sum up, AAS made of silicate activator showed much better initial fresh properties than hydroxide-based AAS mixtures. PNS and LS evidently improved the initial rheological parameters of hydroxide-based mixtures, while both became much less effective in the silicate media.

Effect of HRWRAs on workability retention

Slump, stress growth, and flow curve tests were conducted every 15 minutes in the first hour for each mixture to study the fresh property retention characteristics. The slump value, static/dynamic yield stress, and plastic viscosity with time are shown in Fig. 8, 9, and 10, respectively. In AAS2, the reaction took place more rapidly than in the other mixtures, so it was impossible to perform another group of tests after 45 minutes.

As illustrated in Fig. 8, in the plain AAS mixtures, much lower slump values in AAS2 were detected than that of AAS1. Moreover, AAS1 exhibited a declined slump loss rate over time, while the slump loss in AAS2 continuously accelerated as the reaction progressed. Regarding the effect of PNS and LS, it is evident that both HRWRAs resulted in more slump increments in hydroxide mixtures than in silicate mixtures. In the silicate media, the slump loss curves of AAS3 and AAS5 moved slightly upward compared to AAS1. Nevertheless, PNS and LS remarkably increased the slump value over time in the hydroxide media, with both mixtures maintaining more than 7.87 in. (200 mm) slump value after 30 minutes. The slump curve of AAS6 was obviously flattened compared to AAS2, and a 7.28 in. (185 mm) slump was detected in AAS6 after 60 minutes. In AAS4, the

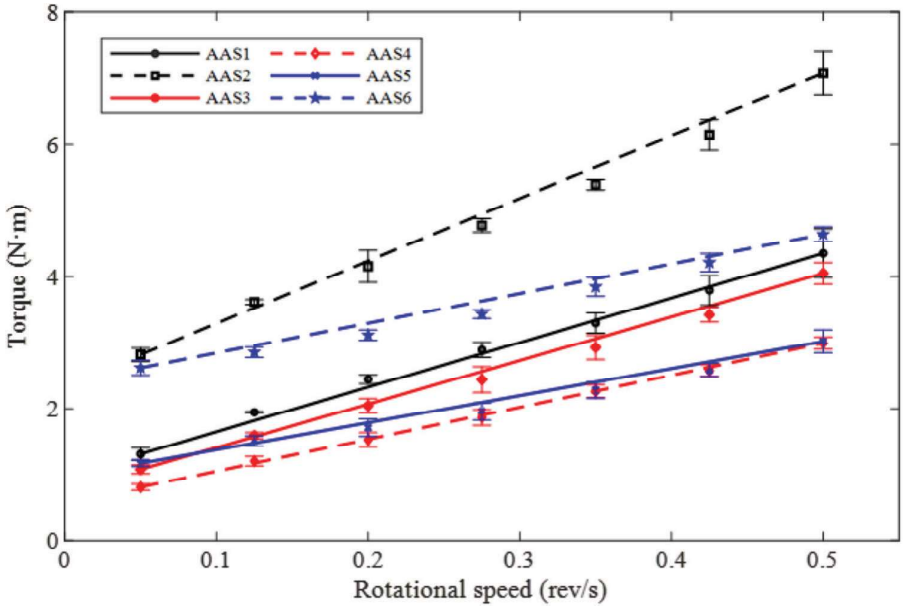

Fig. 6—Flow curves for AAS concretes in torque-rotational speed relationship at 0 minutes.

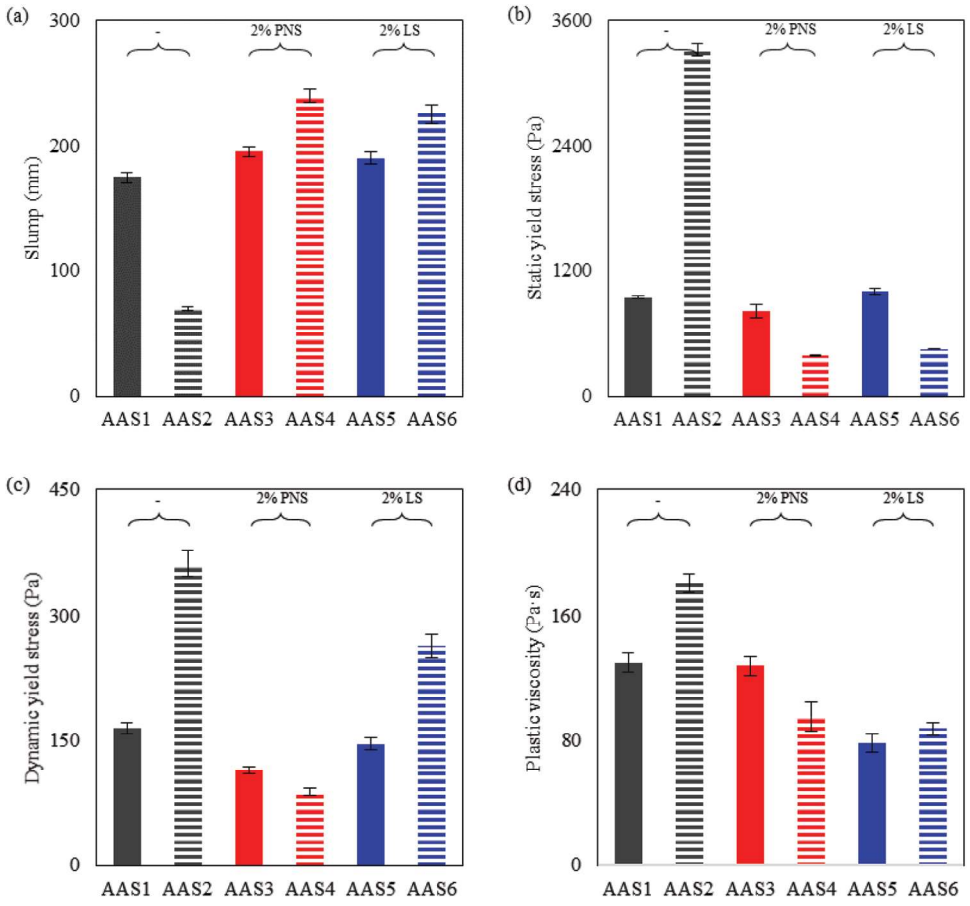

Fig. 7—Initial fresh properties of AAS concretes: (a) slump values; (b) static yield stress; (c) dynamic yield stress; and (d) plastic viscosity. (Note: 1 mm = 0.039 in.; 1 Pa = 1.45 × 10^{-4} psi.)

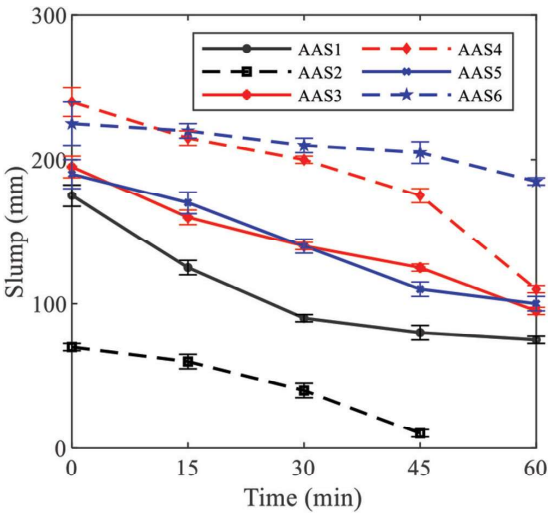

Fig. 8—Slump loss of AAS concretes against time. (Note: 1 mm = 0.039 in.)

slump curve is almost parallel with that of AAS2 from 0 to 45 minutes, followed by an enormous slump loss between 45 and 60 minutes, which is ascribed to the initiation of the acceleration period, as detected by calorimetry at approximately 60 minutes.

The static yield stress evolution of the different AAS concrete mixtures is shown in Fig. 9(a), where AAS2 exhibited the highest static yield stress among all the mixtures. Similar to the observation in the slump tests, the slope of the static yield stress evolution curve became higher after 30 and 45 minutes in AAS2 and AAS4, respectively. By involving silicate species in the activator, the static yield stress in AAS1 steadily increased with the ongoing reaction process, which was much lower compared to AAS2 with time. The result indicates that the inclusion of silicate species in the activator not only provided a fluidizing effect[66] but also slowed down the reaction process. In the silicate media, the addition of both HRWRAs did not result in much difference at the beginning. However, an obvious reduction of static yield stress occurred at 45 and 60 minutes (static yield stress of AAS3 and AAS5 at 60 minutes decreased by approximately 26.1% and 29.1%, respectively, compared to AAS1), which is in agreement with the retardation effect observed by calorimetry measurement. Meanwhile, a significant reduction in static yield stress was observed with time in AAS4 and AAS6 compared to AAS2. The result showed the effectiveness of PNS and LS in hydroxide media.

As shown in Fig. 9(b), AAS2 and AAS4 exhibited a similar development trend in dynamic yield stress compared to static yield stress. The dynamic yield stress of silicate mixtures and AAS6 remained relatively constant within the first hour, while the static yield stress of those mixtures progressively developed with time in the first hour. Such difference might be attributed to the structural breakdown induced by the shear stress exerted during the pre-shear and upward flow curve just before the ramp-down curve, which

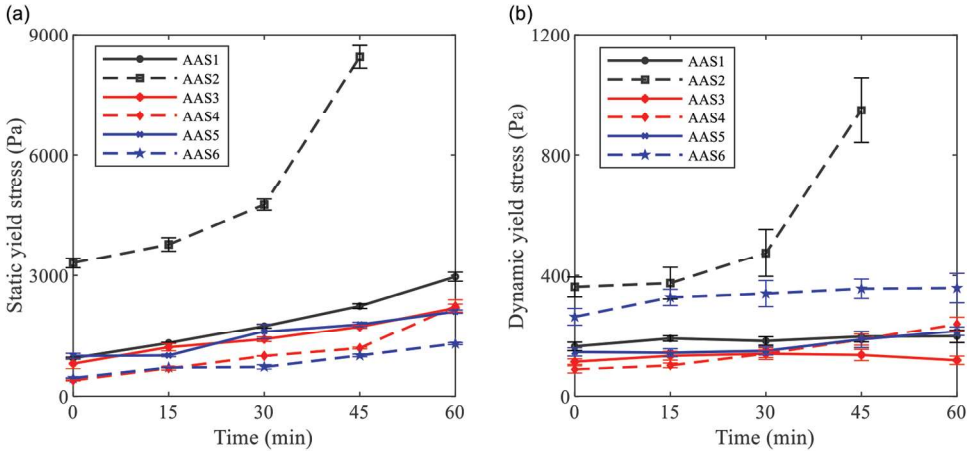

Fig. 9—Yield stress of AAS concretes against time: (a) static yield stress; and (b) dynamic yield stress. (Note: 1 Pa = 1.45 × 10^{-4} psi.)

was used in the dynamic yield stress measurement.[67,68] According to the calorimetry result, all silicate-activated concretes remained in the induction period when rheological tests were performed. Within this period, the concentration of calcium and aluminum ions released from slag particles in the pore solution is way lower with respect to the silicate provided by the activator. In that case, the dissolved Al and Si species in the form of less-polymerized monomers and oligomers[69,70] remained as gels[57] in the pore solution. The precipitation of reaction products takes place only if the solution reached supersaturation, which is supported by Palacios et al.,[13] who observed that a sharp increase in storage modulus of AAS paste occurred together with a drastic drop of the concentration of Al, Si, and Ca in the pore solution. Accordingly, during the first hour when rheology tests were conducted, the structural buildup related to the formation of gel-like intermediate reaction products was not strong enough to withstand the pre-shear applied, so there was no evident dynamic yield stress development. In the hydroxide-activated system, the concentration of multiple elements involved in the polymerization process locally stayed rather consistent around the slag particles because they are all dissolved from the slag. Therefore, the precipitation of reaction products took place continuously along the rapid reaction process.[55] Consequently, the interparticle connections are progressively strengthened by the precipitants, and more free water is trapped in flocs[71,72] as slag particles are better bridged by the reaction products. Therefore, more irreversible structure buildup developed associated with the dynamic yield stress development in AAS2 and AAS4. However, there was no obvious change in those parameters in AAS6, even while it was activated by hydroxide as well. This retardation effect might be linked to the organic sugar content in LS (for example, glucose and sucrose).[73,74] Besides, higher static yield stress was detected in AAS6 with time compared to AAS4, which revealed that LS resulted in more irreversible structural development than PNS in hydroxide media.

Nevertheless, a certain amount of slump loss was detected among all the AAS mixtures with time, which is inconsistent with the dynamic yield stress evolution trend. It is indicated that the shear stress induced by compacting with a tamping rod during the slump test was less strong than the pre-shear induced in the flow curve test and was insufficient to break down the structural development.

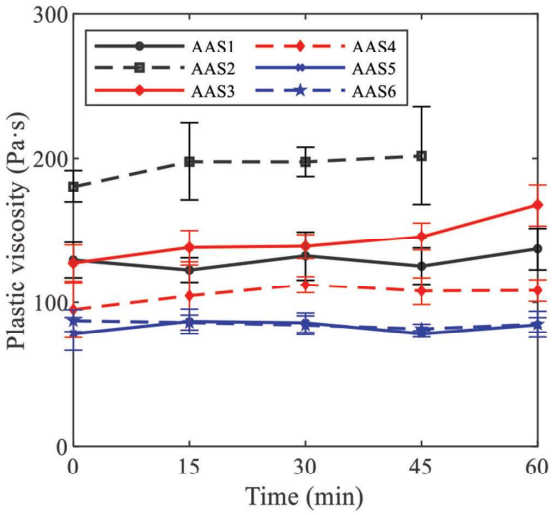

Fig. 10—Plastic viscosity of AAS concretes against time. (Note: 1 Pa = 1.45 × 10^{-4} psi.)

The plastic viscosity in the different AAS concretes remained relatively constant over time, as presented in Fig. 10. The greatest plastic viscosity was detected in AAS2, which might be attributed to the rapid reaction process as well as the higher friction between solid reaction products. Compared to AAS2, the average plastic viscosity from the first hour decreased by approximately 28.3% in AAS1, which once again proved the fluidizing effect of the silicate species in the activator.[66] In the hydroxide media, the average viscosity reduced by approximately 47.4% and 51.7% by applying 2% PNS and LS, respectively. Furthermore, in the silicate media, the viscosity averagely reduced by 39.6% with 2% LS, while PNS, on the contrary, slightly increased the plastic viscosity. Apparently, LS reduced the plastic viscosity of the AAS mixtures in both the silicate and hydroxide media.

Regarding the effect of conventional HRWRAs in AAMs, previous studies pointed out that their ineffectiveness should be blamed on the lower affinity to adsorb on precursors[33] and their unstable nature in aggressive alkaline activators.[35] The

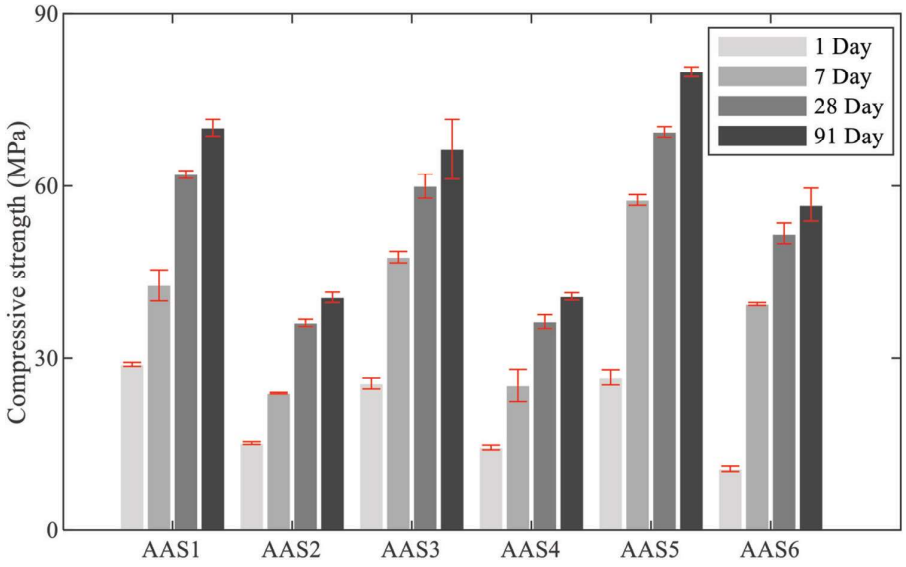

Fig. 11—Compressive strength development of AAS concretes. (Note: 1 MPa = 145 psi.)

results obtained show that both PNS and LS are still effective when sodium hydroxide is applied as the sole alkaline activator. In hydroxide media, HRWRAs remain effective as long as their functional groups[41,77] are stable in a highly alkaline environment. Regardless of the aforementioned stability and adsorption issues, they might still provide a fluidizing effect as smaller fragments[46] or non-absorbing fluid pores.[78] In the case of silicate media, recent rheological studies on silicate-activated AAMs have reported negligible colloidal interactions between precursor particles, whereas the viscous effect that originates from interstitial gels is predominant.[49,79] This can be further supported by the microstructural features reported in Sun et al.,[80] where an interparticle emulsion phase consisting of water droplets and silicate gel networks was detected. Precursor particles were tightly wrapped and dispersed from each other through interstitial silicate gels. Thereby, an enormous water-silicate interface is created,[81,82] leading to highly competitive adsorptions between the interstitial gels and HRWRA molecules.[44] On the other hand, the dispersing effect through electrostatic repulsion and steric hindrance might be inhibited due to the presence of interstitial gels, which resist the interparticle motions through viscous frictions (originated from the interactions between the silicate network and water droplets).[80] It is indicated that the working mechanisms of conventional HRWRAs might not be applicable in silicate-activated AAS mixtures.

To summarize, AAS concretes activated by silicate and hydroxide, in general, exhibited better rheological properties than those activated by hydroxide alone, because the reaction took place rather fast in hydroxide media. Regarding the effect of HRWRAs in AAS concrete, PNS is more effective than LS in hydroxide media; however, none of them effectively improved the rheological properties of silicate-activated AAS concrete. The result is in agreement with previous studies[25,28,33] on paste and mortar levels. Accordingly, PNS might be an ideal HRWRA in AAMs activated by hydroxide to improve workability. On the other hand, further research is required to understand the interaction between HRWRAs and activators. A new generation of HRWRA is required to promote AAM development toward broader field applications.

Compressive strength development

The compressive strength of the AAS concretes at the ages of 1, 7, 28, and 91 days are shown in Fig. 11. In the reference mixture AAS1, 4264 psi (29.4 MPa) 1-day strength and 10,182 psi (70.2 MPa) 91-day strength were obtained. By replacing sodium silicate with sodium hydroxide in AAS2, the compressive strength at all curing ages dropped by approximately 50%. Meanwhile, the silicate species originating from the activator further enhanced the compressive strength development in the late curing stage. The strength increased 1189, 928, and 1523 psi (8.2, 6.4, and 10.5 MPa) from 28 to 91 days in AAS1, AAS3, and AAS5, respectively, while it only increased on average by approximately 725 psi (5 MPa) in the corresponding hydroxide-activated samples.

With the addition of 2% PNS, no evident impact on strength development was observed. Meanwhile, 2% LS resulted in an obvious reduction in 1-day compressive strength in the hydroxide-activated mixtures (AAS6). It has been reported that the LS molecule has a better affinity to bind Ca^{2+},[83] and the addition of LS will result in the formation of calcium complexes.[84] Accordingly, the calcium cations dissolved at the beginning of the reaction process are trapped in complexes; thus, the formation of early-stage reaction products is inhibited. Meanwhile, there was a remarkable strength-enhancing process from 1 to 7 days in AAS5 and AAS6, and their strength improved by 116% and 265% respectively, which is much higher than the corresponding mixtures without HRWRAs during the same period. Eventually, the ultimate compressive strength detected at 91 days increased by 14 and 40% in the two types of alkaline media compared to AAS1 and AAS2. This might be attributed to the calcium content in LS (known as one of the most common positive counter-ions in LS salts[73]), which continuously provides calcium cations to form C-A-S-H gel in the hardened paste. Similar strength enhancement by applying LS has been reported in other AAM[36] and PC mixtures.[85,86]

In either the silicate or hydroxide media, the 1-day compressive strength is in agreement with calorimetry results, and the strength development is proportional to the cumulative heat evolution. However, the compressive strength of the hydroxide-activated samples is generally lower than that of the silicate-activated samples even though the hydroxide-activated mixtures exhibited higher cumulative heat along the reaction process. The result implies the distinctive reaction mechanisms in hydroxide and silicate systems, which have been stressed in previous studies. Regarding the reaction products, larger hydrotalcite crystals have been detected in hydroxide-activated systems,[87] whereas their formations can be blocked due to the presence of silicate content in the activator.[88] Meanwhile, denser C-S-H phases with less chemically bound water were identified around the slag grains in the fast early reaction of the hydroxide-activated mixtures,[89] which inhibited the subsequent ion diffusions. Thereby, the majority of reaction products are attached to the slag surfaces, leading to porous microstructures detected by SEM observations.[89,90] In the case of silicate activation, more nucleation sites are available in the pore solution because the silicate provided by the activator is one of the primary reactants,[91] thereby leading to a much denser and homogeneous microstructure. Accordingly, the spatial arrangement of reaction products and microstructural properties played significant roles in the strength development of AAS.

CONCLUSIONS

In this study, polynaphthalene sulfonate (PNS) and lignosulfonate (LS) high-range water-reducing admixtures (HRWRAs) were applied in alkali-activated slag (AAS) concretes. Their effects on the reaction kinetics, rheology evolution, and strength development of AAS concrete were investigated in hydroxide and silicate media, respectively. The following conclusions could be drawn from the experimental results:

1. In the silicate media, both PNS and LS became less effective in optimizing and retaining the fresh properties.

2. In the hydroxide media, 2% PNS significantly reduced the yield stress and viscosity, and increased the slump values in the first hour. Moreover, LS also showed a retardation effect in the hydroxide mixtures. The second exothermic peak of heat evolution was much delayed, and the cumulative heat release up to 24 hours declined by 50%.

3. The silicate-activated AAS concrete in general showed higher compressive strength than the AAS concrete activated by hydroxide at corresponding curing ages.

4. Two percent PNS did not result in an obvious reduction in compressive strength at all curing ages. However, by applying 2% LS, the early-stage strength development was inhibited due to its retardation effect, while the ultimate strength was enhanced after 91 days.

5. The AAS concrete mixtures made of sodium hydroxide with PNS and LS developed in this study could be regarded as equivalent commercial C30/C40 concrete, with promising slump values and rheological parameters. High-quality AAS concretes could potentially be produced in the near future through proper mixture design with hydroxide activators and market-available HRWRAs.

AUTHOR BIOS

Yubo Sun *is a Doctoral Student at the Magnel-Vandepitte Laboratory in the Department of Structural Engineering and Building Materials at Ghent University, Ghent, Belgium. He received his BS in engineering mechanics from Tianjin University, Tianjin, China, in 2016, and his MS in structural engineering from Delft University of Technology, Delft, the Netherlands, in 2018. His research interests include the rheology of cementitious materials, alkali-activated materials, and supplementary cementitious materials.*

Yaxin Tao *is a Postdoctoral Researcher at Ghent University. He received his BS in road and bridge engineering from Southeast University, Nanjing, Jiangsu, China, in 2015; his MS in tunnel and underground engineering from Tongji University, Shanghai, China, in 2018; and his PhD in civil engineering from Ghent University in 2021. His research interests include the rheology of cementitious materials, cement hydration, and three-dimensional (3-D) printing of concrete.*

A. V. Rahul *is an Assistant Professor at the Indian Institute of Technology Tirupati, Tirupati, Andhra Pradesh, India. Before joining as an assistant professor, he worked as a postdoctoral researcher at the Magnel-Vandepitte Laboratory at Ghent University. His research interests include concrete 3-D printing, the rheology of cement-based materials, cement hydration, and thermodynamics-based constitutive modeling.*

Guang Ye *is an Associate Professor in the Microlab in the Faculty of Civil Engineering and Geosciences at Delft University of Technology, where he received his PhD in 2003. His research interests include material properties at early ages, numerical simulation of microstructure, tomography, and concrete durability.*

Geert De Schutter, *FACI, is a Professor at Ghent University. He is the Head of the Department of Structural Engineering and Building Materials and former RILEM Director of Development. He is the Technical Director of the Magnel-Vandepitte Laboratory. His research interests include concrete technology, hydration and microstructure development, properties of hardening concrete, durability of cementitious materials, self-consolidating concrete, rheology of cementitious materials, and 3-D printing of concrete.*

ACKNOWLEDGMENTS

This paper presents the research results from the DuRSAAM project. The authors wish to acknowledge the financial support from the European Union's Horizon 2020 research and innovation programme (ETN DuRSAAM – H2020-MSCA-ITN-2018-813596).

REFERENCES

1. Damtoft, J. S.; Lukasik, J.; Herfort, D.; Sorrentino, D.; and Gartner, E. M., "Sustainable Development and Climate Change Initiatives," *Cement and Concrete Research*, V. 38, No. 2, Feb. 2008, pp. 115-127. doi: 10.1016/j.cemconres.2007.09.008

2. Provis, J. L., and van Deventer, J. S. J., eds., *Alkali Activated Materials: State-of-the-Art Report, RILEM TC 224-AAM*, Springer, Dordrecht, the Netherlands, 2013.

3. Mishra, J.; Das, S. K.; Krishna, R. S.; Nanda, B.; Patro, S. K.; and Mustakim, S. M., "Synthesis and Characterization of a New Class of Geopolymer Binder Utilizing Ferrochrome Ash (FCA) for Sustainable Industrial Waste Management," *Materials Today: Proceedings*, V. 33, Part 8, 2020, pp. 5001-5006. doi: 10.1016/j.matpr.2020.02.832

4. Longos, A. Jr.; Tigue, A. A.; Dollente, I. J.; Malenab, R. A.; Bernardo-Arugay, I.; Hinode, H.; Kurniawan, W.; and Promentilla, M. A., "Optimization of the Mix Formulation of Geopolymer Using Nickel-Laterite Mine Waste and Coal Fly Ash," *Minerals (Basel)*, V. 10, No. 12, Dec. 2020, Article No. 1144. doi: 10.3390/min10121144

5. Thakur, A. K.; Pappu, A.; and Thakur, V. K., "Synthesis and Characterization of New Class of Geopolymer Hybrid Composite Materials from Industrial Wastes," *Journal of Cleaner Production*, V. 230, Sept. 2019, pp. 11-20. doi: 10.1016/j.jclepro.2019.05.081

6. Rentier, G.; Lelieveldt, H.; and Kramer, G. J., "Varieties of Coal-Fired Power Phase-Out across Europe," *Energy Policy*, V. 132, Sept. 2019, pp. 620-632. doi: 10.1016/j.enpol.2019.05.042

7. Vogl, V.; Åhman, M.; and Nilsson, L. J., "The Making of Green Steel in the EU: A Policy Evaluation for the Early Commercialization Phase," *Climate Policy*, V. 21, No. 1, 2021, pp. 78-92. doi: 10.1080/14693062.2020.1803040

8. Fawer, M.; Concannon, M.; and Rieber, W., "Life Cycle Inventories for the Production of Sodium Silicates," *The International Journal of Life Cycle Assessment*, V. 4, No. 4, July 1999, pp. 207-212. doi: 10.1007/BF02979498

9. Turner, L. K., and Collins, F. G., "Carbon Dioxide Equivalent (CO_2-e) Emissions: A Comparison between Geopolymer and OPC Cement

Concrete," *Construction and Building Materials*, V. 43, June 2013, pp. 125-130. doi: 10.1016/j.conbuildmat.2013.01.023

10. Qing-Hua, C., and Sarkar, S. L., "A Study of Rheological and Mechanical Properties of Mixed Alkali Activated Slag Pastes," *Advanced Cement Based Materials*, V. 1, No. 4, May 1994, pp. 178-184. doi: 10.1016/1065-7355(94)90009-4

11. Chang, J. J., "A Study on the Setting Characteristics of Sodium Silicate-Activated Slag Pastes," *Cement and Concrete Research*, V. 33, No. 7, July 2003, pp. 1005-1011. doi: 10.1016/S0008-8846(02)01096-7

12. Lu, C.; Zhang, Z.; Shi, C.; Li, N.; Jiao, D.; and Yuan, Q., "Rheology of Alkali-Activated Materials: A Review," *Cement and Concrete Composites*, V. 121, Aug. 2021, Article No. 104061. doi: 10.1016/j.cemconcomp.2021.104061

13. Palacios, M.; Gismera, S.; Alonso, M. M.; d'Espinose de Lacaillerie, J. B.; Lothenbach, B.; Favier, A.; Brumaud, C.; and Puertas, F., "Early Reactivity of Sodium Silicate-Activated Slag Pastes and Its Impact on Rheological Properties," *Cement and Concrete Research*, V. 140, Feb. 2021, Article No. 106302.

14. Deir, E.; Gebregziabiher, B. S.; and Peethamparan, S., "Influence of Starting Material on the Early Age Hydration Kinetics, Microstructure and Composition of Binding Gel in Alkali Activated Binder Systems," *Cement and Concrete Composites*, V. 48, Apr. 2014, pp. 108-117. doi: 10.1016/j.cemconcomp.2013.11.010

15. Song, S., and Jennings, H. M., "Pore Solution Chemistry of Alkali-Activated Ground Granulated Blast-Furnace Slag," *Cement and Concrete Research*, V. 29, No. 2, Feb. 1999, pp. 159-170. doi: 10.1016/S0008-8846(98)00212-9

16. Gebregziabiher, B. S.; Thomas, R.; and Peethamparan, S., "Very Early-Age Reaction Kinetics and Microstructural Development in Alkali-Activated Slag," *Cement and Concrete Composites*, V. 55, Jan. 2015, pp. 91-102. doi: 10.1016/j.cemconcomp.2014.09.001

17. Yang, X.; Zhu, W.; and Yang, Q., "The Viscosity Properties of Sodium Silicate Solutions," *Journal of Solution Chemistry*, V. 37, No. 1, Jan. 2008, pp. 73-83. doi: 10.1007/s10953-007-9214-6

18. Provis, J. L., and Bernal, S. A., "Geopolymers and Related Alkali-Activated Materials," *Annual Review of Materials Research*, V. 44, 2014, pp. 299-327. doi: 10.1146/annurev-matsci-070813-113515

19. Garcia-Lodeiro, I.; Palomo, A.; Fernández-Jiménez, A.; and Macphee, D. E., "Compatibility Studies between N-A-S-H and C-A-S-H Gels. Study in the Ternary Diagram Na_2O–CaO–Al_2O_3–SiO_2–H_2O," *Cement and Concrete Research*, V. 41, No. 9, Sept. 2011, pp. 923-931. doi: 10.1016/j.cemconres.2011.05.006

20. Fernández-Jiménez, A., and Puertas, F., "Effect of Activator Mix on the Hydration and Strength Behaviour of Alkali-Activated Slag Cements," *Advances in Cement Research*, V. 15, No. 3, July 2003, pp. 129-136. doi: 10.1680/adcr.2003.15.3.129

21. Aydın, S., and Baradan, B., "Effect of Activator Type and Content on Properties of Alkali-Activated Slag Mortars," *Composites Part B: Engineering*, V. 57, Feb. 2014, pp. 166-172. doi: 10.1016/j.compositesb.2013.10.001

22. Puertas, F.; Varga, C.; and Alonso, M. M., "Rheology of Alkali-Activated Slag Pastes. Effect of the Nature and Concentration of the Activating Solution," *Cement and Concrete Composites*, V. 53, Oct. 2014, pp. 279-288. doi: 10.1016/j.cemconcomp.2014.07.012

23. Puertas, F.; Fernández-Jiménez, A.; and Blanco-Varela, M. T., "Pore Solution in Alkali-Activated Slag Cement Pastes. Relation to the Composition and Structure of Calcium Silicate Hydrate," *Cement and Concrete Research*, V. 34, No. 1, Jan. 2004, pp. 139-148. doi: 10.1016/S0008-8846(03)00254-0

24. Fernández-Jiménez, A., and Puertas, F., "Setting of Alkali-Activated Slag Cement. Influence of Activator Nature," *Advances in Cement Research*, V. 13, No. 3, July 2001, pp. 115-121. doi: 10.1680/adcr.2001.13.3.115

25. Palacios, M.; Banfill, P. F. G.; and Puertas, F., "Rheology and Setting of Alkali-Activated Slag Pastes and Mortars: Effect of Organic Admixture," *ACI Materials Journal*, V. 105, No. 2, Mar.-Apr. 2008, pp. 140-148.

26. Ramachandran, V. S., *Concrete Admixtures Handbook: Properties, Science, and Technology*, Noyes Publications, Park Ridge, NJ, 1984.

27. Yoshioka, K.; Tazawa, E.-I.; Kawai, K.; and Enohata, T., "Adsorption Characteristics of Superplasticizers on Cement Component Minerals," *Cement and Concrete Research*, V. 32, No. 10, Oct. 2002, pp. 1507-1513. doi: 10.1016/S0008-8846(02)00782-2

28. Nematollahi, B., and Sanjayan, J., "Effect of Different Superplasticizers and Activator Combinations on Workability and Strength of Fly Ash Based Geopolymer," *Materials & Design*, V. 57, May 2014, pp. 667-672. doi: 10.1016/j.matdes.2014.01.064

29. Oderji, S. Y.; Chen, B.; Shakya, C.; Ahmad, M. R.; and Shah, S. F. A., "Influence of Superplasticizers and Retarders on the Workability and Strength of One-Part Alkali-Activated Fly Ash/Slag Binders Cured at Room Temperature," *Construction and Building Materials*, V. 229, Dec. 2019, Article No. 116891. doi: 10.1016/j.conbuildmat.2019.116891

30. Laskar, A. I., and Bhattacharjee, R., "Effect of Plasticizer and Superplasticizer on Rheology of Fly-Ash-Based Geopolymer Concrete," *ACI Materials Journal*, V. 110, No. 5, Sept.-Oct. 2013, pp. 513-518.

31. Hardjito, D.; Wallah, S. E.; Sumajouw, D. M. J.; and Rangan, B. V., "On the Development of Fly Ash-Based Geopolymer Concrete," *ACI Materials Journal*, V. 101, No. 6, Nov.-Dec. 2004, pp. 467-472.

32. Aliabdo, A. A.; Abd Elmoaty, A. E. M.; and Salem, H. A., "Effect of Water Addition, Plasticizer and Alkaline Solution Constitution on Fly Ash Based Geopolymer Concrete Performance," *Construction and Building Materials*, V. 121, Sept. 2016, pp. 694-703. doi: 10.1016/j.conbuildmat.2016.06.062

33. Palacios, M.; Houst, Y. F.; Bowen, P.; and Puertas, F., "Adsorption of Superplasticizer Admixtures on Alkali-Activated Slag Pastes," *Cement and Concrete Research*, V. 39, No. 8, Aug. 2009, pp. 670-677. doi: 10.1016/j.cemconres.2009.05.005

34. Tong, S.; Yuqi, Z.; and Qiang, W., "Recent Advances in Chemical Admixtures for Improving the Workability of Alkali-Activated Slag-Based Material Systems," *Construction and Building Materials*, V. 272, Feb. 2021, Article No. 121647. doi: 10.1016/j.conbuildmat.2020.121647

35. Palacios, M., and Puertas, F., "Effect of Superplasticizer and Shrinkage-Reducing Admixtures on Alkali-Activated Slag Pastes and Mortars," *Cement and Concrete Research*, V. 35, No. 7, July 2005, pp. 1358-1367. doi: 10.1016/j.cemconres.2004.10.014

36. Luukkonen, T.; Abdollahnejad, Z.; Ohenoja, K.; Kinnunen, P.; and Illikainen, M., "Suitability of Commercial Superplasticizers for One-Part Alkali-Activated Blast-Furnace Slag Mortar," *Journal of Sustainable Cement-Based Materials*, V. 8, No. 4, 2019, pp. 244-257. doi: 10.1080/21650373.2019.1625827

37. Bakharev, T.; Sanjayan, J. G.; and Cheng, Y.-B., "Effect of Admixtures on Properties of Alkali-Activated Slag Concrete," *Cement and Concrete Research*, V. 30, No. 9, Sept. 2000, pp. 1367-1374. doi: 10.1016/S0008-8846(00)00349-5

38. Kong, D. L. Y., and Sanjayan, J. G., "Effect of Elevated Temperatures on Geopolymer Paste, Mortar and Concrete," *Cement and Concrete Research*, V. 40, No. 2, Feb. 2010, pp. 334-339. doi: 10.1016/j.cemconres.2009.10.017

39. Triwulan, T.; Wigestika, P.; and Ekaputri, J. J., "Addition of Superplasticizer on Geopolymer Concrete," *ARPN Journal of Engineering and Applied Sciences*, V. 11, No. 24, Dec. 2016, pp. 14456-14462.

40. Criado, M.; Palomo, A.; Fernández-Jiménez, A.; and Banfill, P. F. G., "Alkali Activated Fly Ash: Effect of Admixtures on Paste Rheology," *Rheologica Acta*, V. 48, No. 4, May 2009, pp. 447-455. doi: 10.1007/s00397-008-0345-5

41. Laskar, S. M., and Talukdar, S., "Effect of Addition of Fly Ash and Superplasticizer on Ultra-fine Slag Based Geopolymer Mortar," *Recent Advances in Structural Engineering, Volume 1: Select Proceedings of SEC 2016*, A. Rama Mohan Rao and K. Ramanjaneyulu, eds., Springer, Singapore, 2019, pp. 693-702.

42. Weng, C.-H., and Huang, C. P. "Adsorption Characteristics of Zn(II) from Dilute Aqueous Solution by Fly Ash," *Colloids and Surfaces A: Physicochemical and Engineering Aspects*, V. 247, No. 1-3, Oct. 2004, pp. 137-143.

43. Luukkonen, T.; Sarkkinen, M.; Kemppainen, K.; Rämö, J.; and Lassi, U., "Metakaolin Geopolymer Characterization and Application for Ammonium Removal from Model Solutions and Landfill Leachate," *Applied Clay Science*, V. 119, Part 2, Jan. 2016, pp. 266-276. doi: 10.1016/j.clay.2015.10.027

44. Marchon, D.; Sulser, U.; Eberhardt, A.; and Flatt, R. J., "Molecular Design of Comb-Shaped Polycarboxylate Dispersants for Environmentally Friendly Concrete," *Soft Matter*, V. 9, No. 45, Dec. 2013, pp. 10719-10728.

45. RILEM Technical Committee 247-DTA, "RILEM TC 247-DTA Round Robin Test: Mix Design and Reproducibility of Compressive Strength of Alkali-Activated Concretes," *Materials and Structures*, V. 52, No. 5, Oct. 2019, Article No. 99, 13 pp.

46. Kalina, L.; Bílek, V. Jr.; Hrubý, P.; Iliushchenko, V.; Kalina, M.; and Smilek, J., "On the Action Mechanism of Lignosulfonate Plasticizer in Alkali-Activated Slag-Based System," *Cement and Concrete Research*, V. 157, July 2022, Article No. 106822.

47. Puertas, F.; González-Fonteboa, B.; González-Taboada, I.; Alonso, M. M.; Torres-Carrasco, M.; Rojo, G.; and Martínez-Abella, F., "Alkali-Activated Slag Concrete: Fresh and Hardened Behaviour," *Cement and Concrete Composites*, V. 85, Jan. 2018, pp. 22-31. doi: 10.1016/j.cemconcomp.2017.10.003

48. Favier, A.; Habert, G.; d'Espinose De Lacaillerie, J. B.; and Roussel, N., "Mechanical Properties and Compositional Heterogeneities of Fresh Geopolymer Pastes," *Cement and Concrete Research*, V. 48, June 2013, pp. 9-16. doi: 10.1016/j.cemconres.2013.02.001

49. Alnahhal, M. F.; Kim, T.; and Hajimohammadi, A., "Distinctive Rheological and Temporal Viscoelastic Behaviour of Alkali-Activated Fly

Ash/Slag Pastes: A Comparative Study with Cement Paste," *Cement and Concrete Research*, V. 144, June 2021, Article No. 106441.

50. Koehler, E. P., and Fowler, D. W., "Development of a Portable Rheometer for Fresh Portland Cement Concrete," Research Report No. ICAR-105-3F, International Center for Aggregates Research, The University of Texas at Austin, Austin, TX, 2004, 328 pp.

51. Scrivener, K. L., and Nonat, A., "Hydration of Cementitious Materials, Present and Future," *Cement and Concrete Research*, V. 41, No. 7, July 2011, pp. 651-665. doi: 10.1016/j.cemconres.2011.03.026

52. Ravikumar, D., and Neithalath, N., "Reaction Kinetics in Sodium Silicate Powder and Liquid Activated Slag Binders Evaluated Using Isothermal Calorimetry," *Thermochimica Acta*, V. 546, Oct. 2012, pp. 32-43. doi: 10.1016/j.tca.2012.07.010

53. Kashani, A.; Provis, J. L.; Qiao, G. G.; and van Deventer, J. S. J., "The Interrelationship between Surface Chemistry and Rheology in Alkali Activated Slag Paste," *Construction and Building Materials*, V. 65, Aug. 2014, pp. 583-591. doi: 10.1016/j.conbuildmat.2014.04.127

54. Gebregziabiher, B. S.; Thomas, R. J.; and Peethamparan, S., "Temperature and Activator Effect on Early-Age Reaction Kinetics of Alkali-Activated Slag Binders," *Construction and Building Materials*, V. 113, June 2016, pp. 783-793. doi: 10.1016/j.conbuildmat.2016.03.098

55. Zuo, Y., and Ye, G., "Preliminary Interpretation of the Induction Period in Hydration of Sodium Hydroxide/Silicate Activated Slag," *Materials (Basel)*, V. 13, No. 21, Nov. 2020, Article No. 4796, 19 pp. doi: 10.3390/ma13214796

56. Duxson, P., and Provis, J. L., "Designing Precursors for Geopolymer Cements," *Journal of the American Ceramic Society*, V. 91, No. 12, Dec. 2008, pp. 3864-3869. doi: 10.1111/j.1551-2916.2008.02787.x

57. Cao, R.; Zhang, S.; Banthia, N.; Zhang, Y.; and Zhang, Z., "Interpreting the Early-Age Reaction Process of Alkali-Activated Slag by Using Combined Embedded Ultrasonic Measurement, Thermal Analysis, XRD, FTIR and SEM," *Composites Part B: Engineering*, V. 186, Apr. 2020, Article No. 107840. doi: 10.1016/j.compositesb.2020.107840

58. Dimas, D.; Giannopoulou, I.; and Panias, D., "Polymerization in Sodium Silicate Solutions: A Fundamental Process in Geopolymerization Technology," *Journal of Materials Science*, V. 44, No. 14, July 2009, pp. 3719-3730. doi: 10.1007/s10853-009-3497-5

59. Altan, E., and Erdoğan, S. T., "Alkali Activation of a Slag at Ambient and Elevated Temperatures," *Cement and Concrete Composites*, V. 34, No. 2, Feb. 2012, pp. 131-139. doi: 10.1016/j.cemconcomp.2011.08.003

60. Bensted, J., "Some Applications of Conduction Calorimetry to Cement Hydration," *Advances in Cement Research*, V. 1, No. 1, Oct. 1987, pp. 35-44. doi: 10.1680/adcr.1987.1.1.35

61. Bentz, D. P.; Peltz, M. A.; and Winpigler, J., "Early-Age Properties of Cement-Based Materials. II: Influence of Water-to-Cement Ratio," *Journal of Materials in Civil Engineering*, ASCE, V. 21, No. 9, Sept. 2010, pp. 512-517.

62. Trtnik, G.; Turk, G.; Kavčič, F.; and Bosiljkov, V. B., "Possibilities of Using the Ultrasonic Wave Transmission Method to Estimate Initial Setting Time of Cement Paste," *Cement and Concrete Research*, V. 38, No. 11, Nov. 2008, pp. 1336-1342. doi: 10.1016/j.cemconres.2008.08.003

63. Taylor, H. F. W., *Cement Chemistry*, second edition, Thomas Telford Publishing, London, UK, 1997.

64. Chen, X.; Meawad, A.; and Struble, L. J., "Method to Stop Geopolymer Reaction," *Journal of the American Ceramic Society*, V. 97, No. 10, Oct. 2014, pp. 3270-3275.

65. Mahmoodzadeh, F., and Chidiac, S. E., "Rheological Models for Predicting Plastic Viscosity and Yield Stress of Fresh Concrete," *Cement and Concrete Research*, V. 49, July 2013, pp. 1-9. doi: 10.1016/j.cemconres.2013.03.004

66. Alonso, M. M.; Gismera, S.; Blanco, M. T.; Lanzón, M.; and Puertas, F., "Alkali-Activated Mortars: Workability and Rheological Behaviour," *Construction and Building Materials*, V. 145, Aug. 2017, pp. 576-587. doi: 10.1016/j.conbuildmat.2017.04.020

67. Roussel, N., "Steady and Transient Flow Behaviour of Fresh Cement Pastes," *Cement and Concrete Research*, V. 35, No. 9, Sept. 2005, pp. 1656-1664. doi: 10.1016/j.cemconres.2004.08.001

68. Billberg, P. "Form Pressure Generated by Self-Compacting Concrete — Influence of Thixotropy and Structural Behaviour at Rest," PhD thesis, KTH Royal Institute of Technology, Stockholm, Sweden, 2006, 105 pp.

69. Provis, J. L., and van Deventer, J. S. J., "Geopolymerisation Kinetics. 2. Reaction Kinetic Modelling," *Chemical Engineering Science*, V. 62, No. 9, May 2007, pp. 2318-2329. doi: 10.1016/j.ces.2007.01.028

70. Weng, L.; Sagoe-Crentsil, K.; Brown, T.; and Song, S., "Effects of Aluminates on the Formation of Geopolymers," *Materials Science and Engineering: B*, V. 117, No. 2, Mar. 2005, pp. 163-168. doi: 10.1016/j.mseb.2004.11.008

71. Tregger, N. A.; Pakula, M. E.; and Shah, S. P., "Influence of Clays on the Rheology of Cement Pastes," *Cement and Concrete Research*, V. 40, No. 3, Mar. 2010, pp. 384-391.

72. Yang, T.; Zhu, H.; Zhang, Z.; Gao, X.; Zhang, C.; and Wu, Q., "Effect of Fly Ash Microsphere on the Rheology and Microstructure of Alkali-Activated Fly Ash/Slag Pastes," *Cement and Concrete Research*, V. 109, July 2018, pp. 198-207. doi: 10.1016/j.cemconres.2018.04.008

73. Arel, H. Ş., and Aydin, E., "Effects of Ca-, Mg-, K-, and Na-Lignosulfonates on the Behavior of Fresh Concrete," *Construction and Building Materials*, V. 157, Dec. 2017, pp. 1084-1091.

74. Zhang, R.; Xiao, X.; Tai, Q.; Huang, H.; and Hu, Y., "Modification of Lignin and Its Application as Char Agent in Intumescent Flame-Retardant Poly(lactic acid)," *Polymer Engineering & Science*, V. 52, No. 12, Dec. 2012, pp. 2620-2626.

75. Puertas, F.; González-Fonteboa, B.; González-Taboada, I.; Alonso, M. M.; Torres-Carrasco, M.; Rojo, G.; and Martínez-Abella, F., "Alkali-Activated Slag Concrete: Fresh and Hardened Behaviour," *Cement and Concrete Composites*, V. 85, Jan. 2018, pp. 22-31. doi: 10.1016/j.cemconcomp.2017.10.003

76. Assaad, J.; Khayat, K. H.; and Mesbah, H., "Assessment of Thixotropy of Flowable and Self-Consolidating Concrete," *ACI Materials Journal*, V. 100, No. 2, Mar.-Apr. 2003, pp. 99-107.

77. He, Y.; Zhang, X.; Shui, L.; Wang, Y.; Gu, M.; Wang, X.; Wang, H.; and Peng, L., "Effects of PCEs with Various Carboxylic Densities and Functional Groups on the Fluidity and Hydration Performances of Cement Paste," *Construction and Building Materials*, V. 202, Mar. 2019, pp. 656-668. doi: 10.1016/j.conbuildmat.2018.12.216

78. Lange, A., and Plank, J., "Contribution of Non-Adsorbing Polymers to Cement Dispersion," *Cement and Concrete Research*, V. 79, Jan. 2016, pp. 131-136. doi: 10.1016/j.cemconres.2015.09.003

79. Favier, A.; Hot, J.; Habert, G.; Roussel, N.; and d'Espinose de Lacaillerie, J.-B., "Flow Properties of MK-Based Geopolymer Pastes. A Comparative Study with Standard Portland Cement Pastes," *Soft Matter*, V. 10, No. 8, Feb. 2014, pp. 1134-1141. doi: 10.1039/c3sm51889b

80. Sun, Y.; Zhang, S.; Rahul, A. V.; Tao, Y.; Van Bockstaele, F.; Dewettinck, K.; Ye, G.; and De Schutter, G., "Rheology of Alkali-Activated Slag Pastes: New Insight from Microstructural Investigations by Cryo-SEM," *Cement and Concrete Research*, V. 157, July 2022, Article No. 106806. doi: 10.1016/j.cemconres.2022.106806

81. Diamant, H., and Andelman, D., "Kinetics of Surfactant Adsorption at Fluid–Fluid interfaces," *The Journal of Physical Chemistry*, V. 100, No. 32, Aug. 1996, pp. 13732-13742. doi: 10.1021/jp960377k

82. Scamehorn, J. F., ed., *Phenomena in Mixed Surfactant Systems*, ACS Symposium Series No. 311, American Chemical Society, Washington, DC, 1986, 349 pp.

83. Pérez-Nicolás, M.; Duran, A.; Navarro-Blasco, I.; Fernández, J. M.; Sirera, R.; and Alvarez, J. I., "Study on the Effectiveness of PNS and LS Superplasticizers in Air Lime-Based Mortars," *Cement and Concrete Research*, V. 82, Apr. 2016, pp. 11-22. doi: 10.1016/j.cemconres.2015.12.006

84. July, R. "T A B L E 1 Chemical and Mineralogical Composition, and Fineness of Cement and Blending," V. 22, 1992, pp. 1115-1129.

85. Nagrockiene, D.; Pundiene, I.; and Kicaite, A., "The Effect of Cement Type and Plasticizer Addition on Concrete Properties," *Construction and Building Materials*, V. 45, Aug. 2013, pp. 324-331.

86. Topçu, İ. B., and Ateşin, Ö., "Effect of High Dosage Lignosulphonate and Naphthalene Sulphonate Based Plasticizer Usage on Micro Concrete Properties," *Construction and Building Materials*, V. 120, Sept. 2016, pp. 189-197.

87. Wang, S.-D., and Scrivener, K. L., "Hydration Products of Alkali Activated Slag Cement," *Cement and Concrete Research*, V. 25, No. 3, Apr. 1995, pp. 561-571. doi: 10.1016/0008-8846(95)00045-E

88. Schade, T.; Bellmann, F.; and Middendorf, B., "Quantitative Analysis of C-(K)-A-S-H-Amount and Hydrotalcite Phase Content in Finely Ground Highly Alkali-Activated Slag/Silica Fume Blended Cementitious Material," *Cement and Concrete Research*, V. 153, Mar. 2022, Article No. 106706. doi: 10.1016/j.cemconres.2021.106706

89. Ben Haha, M.; Le Saout, G.; Winnefeld, F.; and Lothenbach, B., "Influence of Activator Type on Hydration Kinetics, Hydrate Assemblage and Microstructural Development of Alkali Activated Blast-Furnace Slags," *Cement and Concrete Research*, V. 41, No. 3, Mar. 2011, pp. 301-310. doi: 10.1016/j.cemconres.2010.11.016

90. Zuo, Y., and Ye, G., "Pore Structure Characterization of Sodium Hydroxide Activated Slag Using Mercury Intrusion Porosimetry, Nitrogen Adsorption, and Image Analysis," *Materials (Basel)*, V. 11, No. 6, June 2018, Article No. 1035.

91. Hubler, M. H.; Thomas, J. J.; and Jennings, H. M., "Influence of Nucleation Seeding on the Hydration Kinetics and Compressive Strength of Alkali Activated Slag Paste," *Cement and Concrete Research*, V. 41, No. 8, Aug. 2011, pp. 842-846. doi: 10.1016/j.cemconres.2011.04.002